Control Engineering Practice 20 (2012) 805–815

Contents lists available at SciVerse ScienceDirect

Control Engineering Practice

journal homepage: www.elsevier.com/locate/conengprac

A parameter-varying filtered PID strategy for air–fuel ratio control of spark ignition engines

Behrouz Ebrahimi [a], Reza Tafreshi [a,*], Houshang Masudi [a], Matthew Franchek [b], Javad Mohammadpour [b], Karolos Grigoriadis [b]

[a] Mechanical Engineering Program, Texas A&M University at Qatar, Doha 23874, Qatar
[b] Department of Mechanical Engineering, University of Houston, Houston, TX 77204, USA

ARTICLE INFO

Article history:
Received 30 September 2011
Accepted 10 April 2012
Available online 2 May 2012

Keywords:
AFR control
Time-varying delay
Non-minimum phase system
Dynamic compensator
Spark ignition engine

ABSTRACT

In this paper, a new synthesis method is presented to control air–fuel ratio (AFR) in spark ignition engines to maximize the fuel economy while minimizing exhaust emissions. The major challenge in the control of AFR is the time-varying delay in the control loop which restricts the application of conventional control techniques. In this paper, the time-varying delay in the system dynamics is first approximated by Padé approximation to render the system dynamics into non-minimum phase characteristics with time-varying parameters. Application of parameter-varying dynamic compensators is invoked to retrieve unstable internal dynamics. The associated error dynamics is then utilized to construct a filtered PID controller combined with a parameter-varying dynamic compensator to track the desired AFR command using the feedback from the universal exhaust gas oxygen sensor. The proposed method achieves desired dynamic properties independent of the matched disturbances. It also accommodates the unmatched perturbations due to the dynamic compensator features. The results of applying the proposed method to experimental numerical data demonstrate the closed-loop system stability and performance against time-varying delay, canister purge disturbances and measurement noise for both port fuel injection engines and lean-burn engines.

1. Introduction

Spark ignition engines are commonly equipped with electronic control systems whose task is to provide desired air–fuel ratio (AFR) signal tracking to improve the fuel economy and reduce exhaust emissions. The engine control system maintains the AFR to be close to the stoichiometric value as an index of maximum catalytic convertor efficiency. Unfortunately, performance of the catalytic convertors depends significantly on the precise value of the AFR. For instance, exceeding the stoichiometric value by 1% results in about 50% higher NO_x emissions while receding the stoichiometric value by 1% dramatically increases CO and HC levels (Manzie, Palaniswami, Ralph, Watson, & Yi, 2002). In addition to the emission concerns, regulated AFR according to the stoichiometric value can also improve the fuel economy and provide efficient torque demands. However, the wide range of engine operating conditions, the inherent nonlinearities of the combustion process, the large modeling uncertainties and parameter variations make the control system design a challenging task. Furthermore, the time-varying delay in the spark ignition (SI) engines poses additional challenges to the AFR control problem.

There have been numerous research efforts on AFR control characteristics over the years. Sliding mode control systems have been extensively investigated for both narrowband binary and wideband dynamics of the Universal Exhaust Gas Oxygen (UEGO) sensors based on the sliding manifolds constructed on the AFR provisions (Cho & Hedrick, 1988; Pace & Zho, 2009). Cho and Hedrick presented switching surface according to the stoichiometric value with a great insight into the chattering analysis by employing conventional sliding mode theory (Cho & Hedrick, 1988). However, attractiveness of the switching surface was only guaranteed for a boundary layer in the vicinity of the surface depending directly on the time delay. This, in turn, implied that for a large time delay there would be considerable tracking error. In a follow-up paper an observer-based sliding mode control was proposed to improve the chattering considerably (Choi & Hedrick, 1998). A second-order continuous sliding mode control was proposed in Wang and Yu (2007) for chattering suppression by integrating a discontinuous control and a delay free switching surface. In addition, adaptive mechanisms for AFR control and engine parameter estimation have been presented in Turin and

* Corresponding author.
E-mail address: reza.tafreshi@qatar.tamu.edu (R. Tafreshi).

0967-0661/$ - see front matter © 2012 Elsevier Ltd. All rights reserved.
http://dx.doi.org/10.1016/j.conengprac.2012.04.001

Geering (1995) and Ault, Jones, Powell, and Franklin (1994). Application of direct adaptive control has been also presented based on the positive forecast idea which in fact is a counterpart to classical Smith predictors (Yildiz, Annaswamy, Yanakiev, & Kolmanovski, 2010). The presented method in this paper would result in reduced tuning and calibration effort compared to the method in Yildiz et al. (2010). In Manzie et al. (2002) a model predictive control based on a radial basis function network was presented to maintain a proper performance level against engine changing characteristics.

Many of the current production control systems are based on the gain-scheduling approach to design feedforward and/or feedback control system by constructing lookup tables (Apkarian & Adams, 1998). Although the method may be a laborious process in terms of calibration and tuning with burden of calculations in the control hardware, it can be done for nonlinear and parameter-dependent systems to provide stability and desired performance. The gain-scheduling control method represents a parameter-varying control upon the operating envelope of the engine using a grid of operating points and then schedules the control gains for the engine differential inclusion under continuously varying conditions. A more systematic way for gain-scheduling control design for dynamic systems with varying operating conditions is the Linear Parameter-Varying (LPV) control method. An LPV gain-scheduling controller was designed for the AFR control of a lean-burn engine in Zhang, Grigoriadis, Franchek, and Makki (2007) which exploited the use of a prefilter to extend the closed-loop AFR tracking bandwidth by presenting an explicit parameterization of the controller.

On the other hand, proportional–integral–derivative (PID) controllers are by far the most dominant control design approach in practice. Recent research trends in the PID control are well summarized in Li, Ang, and Chong (2006). In the recent years, with the advent of compact and powerful digital processors, various algorithms have been integrated with PID digital control systems (Chang & Jung, 2009; Kwiatkowski, Werner, Blath, Ali, & Schulalbers, 2009). A PID controller for the AFR control using estimated cylinder peak pressure and its location by means of a multi-layer feedforward neural network has been presented in Yoon, Park, Sunwoo, Ohm, and Yoon (2000), where the estimated peak pressure and its location have been used to identify the AFR control parameters. An adaptive delay compensated PID controller for the AFR control with parameters tuned using a lookup table has been developed in Franceschi, Mucke, Jones, and Makki (2007); however, the derivative term has been canceled due to the noisy signals out of the UEGO sensor.

The general approaches to control the AFR include inner/outer control loops, where the outer-loop generates a reference AFR command for the inner-loop based on the three-way catalyst (TWC) states while the inner-loop maintains the AFR upstream of the TWC as close as possible to the desired AFR using the feedgas output measured by the UEGO sensor. For the inner control loop the time-varying delay is the key parameter in the AFR control that imposes a limitation on the bandwidth of the AFR feedback loop by decreasing the phase margin. The inner control loop's delay mainly consists of two parts: the cycle delay due to the four strokes of the engine and the exhaust gas transport delay caused by the exhaust gas to flow from the exhaust valve to the tailpipe UEGO sensor. Consequently, the delay depends on the engine operating condition in terms of the engine speed and air mass flow. In this work, the inner-loop of the AFR control system with time-varying delay will be approximated by a first order Padé approximation to transform the system into a non-minimum phase configuration with time-varying parameters. The corresponding non-minimum phase dynamics will be compensated by a proper parameter-varying compensator in a systematic and straightforward framework. Then, a parameter-varying filtered PID controller will be constructed based on the compensated tracking error. The closed-loop system performance will be evaluated against variable time delay, uncertain plant behavior and disturbances introduced either by purging the fuel vapor from the carbon canister or air charge estimation error. The contributions of the present paper are as follows: (i) the design of a parameter-varying filtered PID control scheme based on a parameter-varying dynamic compensation which is robust against matched and unmatched perturbations for the systems with variable input delay; (ii) development of a general design approach for the parameter-varying dynamic compensator to stabilize the system internal dynamics; (iii) examination of the applicability of the proposed control to both delayed and non-minimum phase system with no need to tune the PID control gains.

Section 2 will address the engine model. In Section 3, the control design approach pertaining control objectives, delay interpretation and design procedure will be presented. Section 4 will outline simulations based on the experimental data and Section 5 will conclude the paper.

2. System model for AFR dynamics

The open-loop block diagram of the plant is depicted in Fig. 1. It consists of the fueling dynamics, the UEGO sensor and the TWC downstream the engine. The characteristics of the fueling system are quite complicated and depend on various parameters such as injection timing, spray pattern, port geometry, and intake manifold temperature. Implementation of the fueling system model with all these impacting factors is a challenging task. A schematic of fueling chamber including vaporized and fluid fuel is shown in Fig. 2. The scheme by Aquino is perhaps the most widely used fueling system model in SI engine control systems (Aquino, 1989). The proposed model has been shaped based on a simple description of the throttle body injection system expressed as

$$\ddot{m}_{fo}+\frac{1}{\tau_f}\dot{m}_{fo}=(1-X)\ddot{m}_{fi}+\frac{1}{\tau_f}\dot{m}_{fi} \tag{1}$$

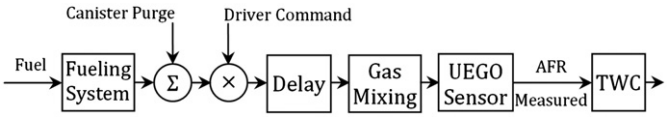

Fig. 1. Plant open-loop block diagram representation.

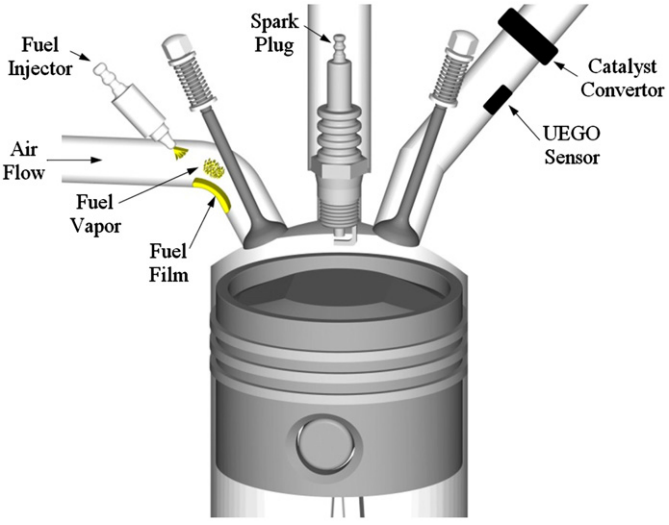

Fig. 2. Schematic of air–fuel path in SI engine.

where X is a fraction of injected fuel that forms a wet film on the walls, τ_f is the time constant for the evaporated fuel from the wet wall, $\dot{m}_{fi}$ and $\dot{m}_{fo}$ are injected fuel flow rate into the fueling chamber and output flow rate delivered into the ignition chamber, respectively. The commanded fuel flow rate is calculated using the cylinder air charge per engine cycle $\dot{m}_a$ and the commanded AFR (AFR^{com}) as $\dot{m}_{fi}=\dot{m}_a/AFR^{com}$. Hence, the open-loop engine model is characterized by the commanded AFR as the input and the measured AFR (by the UEGO sensor) as the system output. As a common practice in experimental settings, a feedforward fueling based on a proper estimation of the fueling system parameters is used to compensate for the fuel wall wetting effect in the intake manifold. Estimation approaches based on the least-squares method to obtain the parameters X and τ_f have been presented in Jones, Ault, Franklin, and Powell (1994) and Wu, Chen, Hsieh, and Ke (2009).

The time-varying delay during the engine operating envelope is the major difficulty to achieve the desired tracking performance. The engine time delays are mainly classified into cycle delay τ_c and exhaust gas transport delay τ_g. The former is identified approximately as one engine cycle due to the four strokes of the engine and the latter is considered as the time that it takes for the exhaust gas flow from the exhaust valve to reach the tailpipe UEGO sensor (Zhang et al., 2007). Thus, the cycle delay is identified as

$$\tau_c=\frac{720}{(360/60)n}=\frac{120}{n} \tag{2}$$

where n is the engine speed in *rpm*. As for the gas transport delay, it varies mainly with the air flow rate and may be approximated for an average exhaust temperature by

$$\tau_g=\frac{\alpha}{\dot{m}_a} \tag{3}$$

where α is a constant identified using the experimental data and estimation results. Hence, the overall time delay is given by $\tau=\tau_c+\tau_g$. The sensor dynamics for the UEGO is modeled by a first order lag $G(s)=1/(\tau_s s+1)$, where τ_s is the sensor time constant. Thus, the system open-loop including UEGO dynamics and the overall delay is considered as

$$\tau_s\dot{y}(t)+y(t)=u(t-\tau) \tag{4}$$

where $y(t)$ and $u(t)$ are the measured and input AFR, respectively.

3. Control design procedure

3.1. Objectives and challenges

The structure of the closed-loop system of this paper is shown in Fig. 3. Air-path dynamics includes the amount of air mass flow that contributes to the combustion process through the throttle valve voltage, V_{MAF}, while the fuel-path dynamics consists of the amount of fuel mass flow entering the combustion process. An extensive study on air and fuel characteristics along with a feedforward approach to explore transient air-path and fuel-path dynamics has been reported in Franchek, Mohrfeld, and Osburn (2006). As a common practice in experimental settings, there is a feedforward fueling to compensate for the fuel-path dynamics using the properly estimated parameters of Eq. (1), i.e., X and τ_f. In designing the control system, a similar methodology is used and the effects of uncompensated fuel-path dynamics is considered in Section 4. The design objective is to track the desired AFR in the presence of matched and unmatched disturbances such as canister purge, open-loop perturbations and unmodeled dynamics effects. The controller should also be able to track the reference AFR command with zero tracking error. As already pointed out in Section 1, the main obstacle in designing an AFR controller is the delay and its variation during different engine operating conditions which restricts the closed-loop system bandwidth. In order to achieve a fast regulation response for the closed-loop system a desired bandwidth greater than 1 rad/s ($\omega_B>1$ rad/s) is empirically selected in this study. The control system should also be robust against unmatched perturbations, as well as matched disturbances. Furthermore, the control system structure should be simple in order to be easily implemented in practical settings.

3.2. Delay and internal dynamics

The pure time delay may be approximated by Padé approximation resulting in a finite dimensional closed form solution

$$e^{-\tau s}\cong\frac{\sum_{i=0}^{j}(-1)^i\frac{(2j-i)!}{(j-i)!i!}(\tau s)^i}{\sum_{i=0}^{j}\frac{(2j-i)!}{(j-i)!i!}(\tau s)^i} \tag{5}$$

where τ is the overall time-varying delay consisting of cycle delay and exhaust gas transport delay. In this paper, a first order Padé approximation is used. Higher order approximation increases the complexity of the system, and hence increases the computational cost. The overall system followed by the approximation can be written as:

$$\frac{Y(s)}{U(s)}\cong\frac{1-\frac{\tau}{2}s}{\left(1+\frac{\tau}{2}s\right)(1+\tau_s s)} \tag{6}$$

Eq. (6) exhibits delay-dependent non-minimum phase characteristics due to the presence of a zero in the right-hand plane caused by the delay. It should be noted that although the approximation renders the infinite dimensional dynamics into the finite dimensional, it still has the bandwidth limitation inherited by the non-minimum phase configuration. The state-space representation of (6) is as follows:

$$\begin{cases}\dot{x}_1(t)=x_2(t)\\ \dot{x}_2(t)=-a_0(\rho)x_1(t)-a_1(\rho)x_2(t)+u(t)\\ y(t)=b_0(\rho)x_1(t)+b_1(\rho)x_2(t)\end{cases} \tag{7}$$

where $\rho=\tau^{-1}$ is the variable parameter in term of time-varying delay and $a_0(\rho)=b_0(\rho)=2\tau_s^{-1}\rho$, $a_1(\rho)=2\rho+\tau_s^{-1}$, and $b_1(\rho)=-\tau_s^{-1}$ are corresponding parameter-dependent coefficients. The relative degree of the system (7) is $r=1$, which states

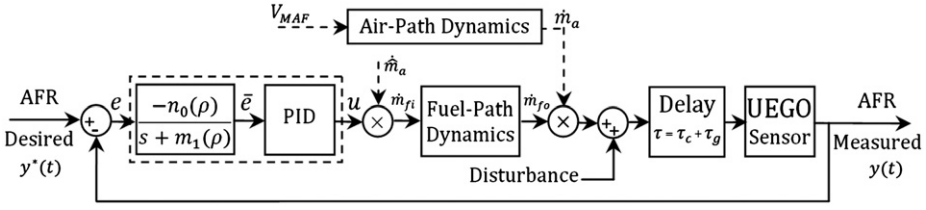

Fig. 3. Closed-loop controller structure.

that the stability of the system depends on the stability of the internal dynamics or alternatively zero dynamics. Internal dynamics along with input/output dynamics of the system may be obtained by the normal form transformation $W=\Phi(x(t))$ in which (Isidori, 1995)

$$W=[\xi(t)\ \eta(t)]^T,\quad \Phi(x)=[y(t)\ x_1(t)]^T \tag{8}$$

Corresponding input/output and internal dynamics can be obtained by using Lie notation as

$$\dot{\eta}(t)=\mathcal{L}_f\Phi(x(t))$$

$$\dot{\xi}(t)=\mathcal{L}_f h(x(t))+\mathcal{L}_g h(x(t))u(t) \tag{9}$$

where $f(x(t))=[x_2(t)\ -a_0(\rho)x_1(t)-a_1(\rho)x_2(t)]^T$, $g(x(t))=[0\ 1]^T$, $h(x(t))=b_0(\rho)x_1(t)+b_1(\rho)x_2(t)$ and Φ is found such that $\mathcal{L}_g\Phi(x(t))=0$. Hence, the internal dynamics and input/output pairs are obtained as

$$\begin{cases}\dot{\eta}(t)=a_{11}(\rho)\eta(t)+a_{12}(\rho)\xi(t)\\ \dot{\xi}(t)=a_{21}(\rho)\eta(t)+a_{22}(\rho)\xi(t)+\beta(\rho)u(t)\\ y(t)=\xi(t)\end{cases} \tag{10}$$

where $a_{11}(\rho)=2\rho$, $a_{12}(\rho)=-\tau_s$, $a_{21}(\rho)=8\tau_s^{-1}\rho^2+4\tau_s^{-2}\rho$, $a_{22}(\rho)=-4\rho-\tau_s^{-1}$, and $\beta(\rho)=-\tau_s^{-1}$ are corresponding coefficients according to the performed transformation. The unstable eigenvalue for the zero dynamics based on $\xi=0$ is equal to 2ρ which alternatively represents instability of the internal dynamics of the system (10) for all the positive time delays. In the sequel, a systematic procedure is presented to design a compensator to stabilize the internal dynamics.

3.3. Control and compensator

Let us consider a PID controller for the system (10) as

$$u(t)=k_p e(t)+k_d\dot{e}(t)+k_i\int_0^t e(\sigma)\,d\sigma \tag{11}$$

where $e(t)=y^*(t)-\xi(t)$, $y^*(t)$ is the reference AFR and k_i, k_p, k_d are the control's integral, proportional and derivative gains, respectively. As previously stated, the non-minimum phase characteristics caused by the unstable zero from the delay in the input restricts direct application of (11) as a control input. Even, robust nonlinear control techniques such as sliding mode control with highly defined bandwidth for the switching manifolds (Shkolnikov & Shtessel, 2001) are overwhelmed by the instability of the internal dynamics. This imperfection allows the PID control to provide neither the output tracking error dynamics with given eigenvalue placement nor stabilization of the system internal dynamics. The design approach for a class of second order non-minimum phase systems with the system total relative degree $r=1$ can be generalized as

$$\begin{cases}\dot{\eta}(t)=a_{11}(\rho)\eta(t)+a_{12}(\rho)\xi(t)+\phi_\eta(t)\\ \dot{\xi}(t)=a_{21}(\rho)\eta(t)+a_{22}(\rho)\xi(t)+\beta(\rho)u(t)+\phi_\xi(t)\\ y(t)=\xi(t)\end{cases} \tag{12}$$

where $\xi(t),\eta(t)\in\Re$ are the output and internal dynamics state, respectively, and $\phi_\xi(t)$ is a bounded nonlinear uncertain term.

Assumption 1. Assume that $\phi_\eta(t)$ is a bounded smooth external unmatched disturbance whose nth order time derivative (n is a non-zero and positive number) is zero, i.e., $d^n/dt^n\phi_\eta(t)\equiv 0$. Also, assume that the same assumption is valid for the reference input $y^*(t)$ and $d^n/dt^n y^*(t)\equiv 0$ for $n>0$.

Assumption 2. It is assumed that the pair $(a_{11}(\rho),a_{12}(\rho))$ is controllable, i.e., $a_{12}(\rho)\neq 0$.

To obtain the zero dynamics of the system, the internal dynamics may be solved for the null output of the system. This would result in an unstable eigenvalue for the first equation in (12), i.e., $a_{11}(\rho)>0$. In order to stabilize the unstable internal dynamics and reduce the effect of unmatched disturbances on the steady-state tracking error, a parameter-varying dynamic compensator operating on the tracking error and unstable internal dynamics is proposed as

$$\sum_{i=0}^{n-1}n_i(\rho)\frac{d^i}{dt^i}e(t)+\left(\frac{d^{n+1}}{dt^{n+1}}+m_n(\rho)\frac{d^n}{dt^n}\right)\eta(t)=0 \tag{13}$$

where $m_n(\rho)$ and $n_i(\rho)$ are parameter-dependent coefficients that should be determined. Substituting (13) into the first equation in (12) and using $\xi(t)=y^*(t)-e(t)$ yields

$$\left[\frac{d^{n+1}}{dt^{n+1}}+m_n(\rho)\frac{d^n}{dt^n}-a_{12}^{-1}(\rho)\sum_{i=0}^{n-1}n_i(\rho)\left(\frac{d^{i+1}}{dt^{i+1}}-a_{11}(\rho)\frac{d^i}{dt^i}\right)\right]e(t)$$
$$=a_{12}^{-1}(\rho)\left(\frac{d^{n+1}}{dt^{n+1}}+m_n(\rho)\frac{d^n}{dt^n}\right)\overline{\phi}(t) \tag{14}$$

where $\overline{\phi}(t)=a_{12}(\rho)y^*(t)+\phi_\eta(t)$. Based on Assumption 1, the term in the right hand side of (14) is vanished and zero steady state tracking error is achieved. Thus, (14) can be rewritten as

$$\left[\frac{d^{n+1}}{dt^{n+1}}+m_n(\rho)\frac{d^n}{dt^n}-a_{12}^{-1}(\rho)\sum_{i=0}^{n-1}n_i(\rho)\left(\frac{d^{i+1}}{dt^{i+1}}-a_{11}(\rho)\frac{d^i}{dt^i}\right)\right]e(t)=0 \tag{15}$$

Now, let the desired system of differential equation for the output tracking error be expressed as

$$\left(\frac{d^{n+1}}{dt^{n+1}}+\sum_{i=0}^{n}c_i\frac{d^i}{dt^i}\right)e(t)=0 \tag{16}$$

where c_i's specify the desired eigenvalues of the error system. By rearranging Eq. (15) in descending order of derivatives and equating the corresponding coefficients in Eq. (15) and (16), one can obtain $n_i(\rho)=a_{12}(\rho)\sum_{j=0}^{i}a_{11}^{j-i-1}(\rho)c_j$ and $m_n(\rho)=c_n+\sum_{j=0}^{n-1}a_{11}^{j-n}(\rho)c_j$. Thus, (13) can be rewritten as

$$a_{12}(\rho)\sum_{i=0}^{n-1}\sum_{j=0}^{i}a_{11}^{j-i-1}(\rho)c_j\frac{d^i}{dt^i}e(t)$$
$$+\left(\frac{d^{n+1}}{dt^{n+1}}+c_n\frac{d^n}{dt^n}+\sum_{j=0}^{n-1}a_{11}^{j-n}(\rho)c_j\frac{d^n}{dt^n}\right)\eta(t)=0 \tag{17}$$

Substitution of the compensator (17) into the state-space representation (7) gives the following filtered PID control as

$$u(t)=a_1(\rho)\overline{e}(t)+\dot{\overline{e}}(t)+\int_0^t a_0(\rho)\overline{e}(\sigma)\,d\sigma \tag{18}$$

where $\overline{e}$ is the filtered error based on the dynamic compensator (17) and is obtained as

$$\left(\frac{d^n}{dt^n}+c_n\frac{d^{n-1}}{dt^{n-1}}+\sum_{j=0}^{n-1}a_{11}^{j-n}(\rho)c_j\frac{d^{n-1}}{dt^{n-1}}\right)\overline{e}(t)=-a_{12}(\rho)\sum_{i=0}^{n-1}\sum_{j=0}^{i}a_{11}^{j-i-1}(\rho)c_j\frac{d^i}{dt^i}e(t) \tag{19}$$

4. Results and discussion

For the engine dynamics, the zero dynamics in (10) matches that in (12) and the internal dynamics is presented by

$$\dot{\eta}(t)=a_{11}(\rho)\eta(t)+a_{12}(\rho)\xi(t)+\phi_\eta(t) \tag{20}$$

Eq. (20) may be rewritten as

$$\dot{\eta}(t)=2\rho\eta(t)-\tau_s[y^*(t)-e(t)]+\phi_\eta(t) \tag{21}$$

where $y^*(t)$ is the reference AFR. Eq. (21) can be further expressed in the following form:

$$\dot{\eta}(t) = 2\rho\eta(t) + \tau_s e(t) + \overline{\phi}_\eta(t) \tag{22}$$

where $\overline{\phi}_\eta(t) = -\tau_s y^*(t) + \phi_\eta(t)$. According to Section 3 and assuming that $\overline{\phi}_\eta(t) = 0$, the following second order dynamic equation is proposed for the unstable internal dynamics:

$$\left[\frac{d^2}{dt^2} + m_1(\rho)\frac{d}{dt}\right]\eta(t) + n_0(\rho)e(t) = 0 \tag{23}$$

Hence, the output tracking error in (22) can be described as

$$\left[\left(\frac{d}{dt} - 2\rho\right)n_0(\rho) + \tau_s\left(\frac{d^2}{dt^2} + m_1(\rho)\frac{d}{dt}\right)\right]e(t) = 0 \tag{24}$$

As a first illustrative case, consider a constant time delay of the engine as $\tau = 0.5$ s ($\rho = 2$) and the sensor lag $\tau_s = 0.4$ s (Yildiz et al., 2010). Unlike the time-varying delay, the constant delay reconfigures the time-varying control system into a fixed-gain controller with gains calculated at the given delay τ. Later in this section, the performance of the parameter-varying control (18) is discussed in detail. However, it is shown that the proposed control law can be used as a fixed-gain control system for the time-varying delay as well.

In order to minimize the transient overshoots and undershoots corresponding to the non-minimum phase system, the integral of time multiplied by absolute value of tracking error criterion (ITAE: $J = \int_0^\infty t|e(t)|\,dt$) is used to obtain the desired second order error dynamics as $\ddot{e} + 1.4\omega_n\dot{e} + \omega_n^2 e = 0$, where ω_n is the desired natural frequency. If $\omega_n = 2$ rad/s the bandwidth of the closed-loop system will be $\omega_B > 2$ rad/s. Thus, the corresponding coefficients in (23) can be found as $m_1 = 3.8$ and $n_0 = -0.4$. Substitution of (23) into (7) yields the corresponding filtered PID controller with already known control gains as

$$u(t) = a_1(\rho)\overline{e}(t) + \dot{\overline{e}}(t) + \int_0^t a_0(\rho)\overline{e}(\sigma)\,d\sigma \tag{25}$$

where $a_0(\rho) = a_0(2) = 10$, $a_1(\rho) = a_1(2) = 6.5$ (Eq. (7)) and $\overline{e}(t)$ is the compensated error based on the dynamic compensator in (23) and is obtained as

$$\dot{\overline{e}}(t) + 3.8\overline{e}(t) = 0.4e(t) \tag{26}$$

The controller gains are obtained directly from the substitution of the controller (11) into the system dynamics (7) that yields respective control gains as $k_p = a_1(\rho)$, $k_d = 1$, $k_i = a_0(\rho)$. Hence, the achieved controller does not require to be tuned over the engine operating envelope. The compensated internal dynamics is shown in Fig. 4 for various delays. The resulting gain margin for $\tau = 0.5$ s is 12 dB and the phase margin is 60°. The achieved bandwidth is 2.3 rad/s which is greater than the desired value ($\omega_B > 1$ rad/s). The simulations are performed in Simulink® using Runge–Kutta ODE4 numerical integration. Also the AFR is normalized using the stoichiometric value of 14.7. The control system performance for the non-minimum phase system representation of the engine is shown in Fig. 5(a), where the overshoots and undershoots illustrate the non-minimum phase behavior of the system. The percentage of the overshoot and undershoot for the reference output is less than 2%. Corresponding tracking error has been plotted in Fig. 5(b). The simulation of the proposed control scheme on the actual time delay model of the engine has been demonstrated in Fig. 6(a), where the overshoot percentage is zero and the time constant is less than 0.8 s. Fig. 6(b) shows the corresponding tracking error for the command signal and approximated non-minimum phase system.

In order to evaluate the control performance against open-loop disturbances including fuel injector uncertainty and canister purge, the disturbance profile in Fig. 7 is added to the AFR input and the corresponding AFR tracking and its error profile are shown in Fig. 8(a) and (b), respectively. In practice, the estimated time delay does not exactly match the actual total engine delay. In order to evaluate the control performance against such imperfections, additional simulations are carried out for delay variation that may arise because of the delay estimation techniques. The results in Fig. 9 are presented for three cases: (i) nominal delay; (ii) 20% time delay overestimation; (iii) 20% time delay underestimation. A detailed view is also shown in Fig. 10, where the dashed line is the reference AFR. The solid line is the overestimated time delay, the dash-dotted line corresponds to the underestimated time delay, and the dotted line is the engine output AFR for the nominal time delay. It is shown that the system is robust against delay variation with zero steady state tracking error. However, for large delays the controller exhibits overshoot while attenuating the disturbance. This is originated from the phase shift caused by the larger delay that makes the system damping smaller and thus allowing for transient overshoot. Moreover, the system response is evaluated in the presence of measurement noise that might be produced by the UEGO sensor. The noise is modeled as a white noise signal with intensity of 10^{-4} that

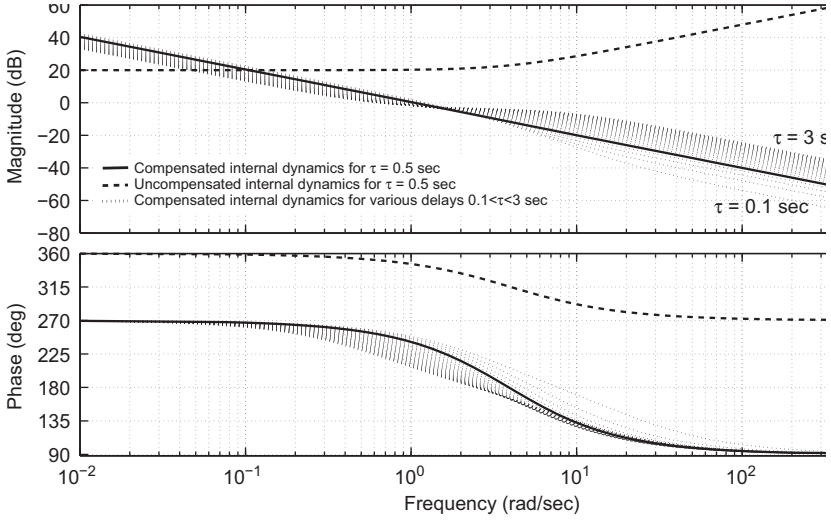

Fig. 4. Compensated internal dynamics for various delay magnitudes. For $\tau = 0.5$ s: $PM = 60°$, $GM = 12$ dB.

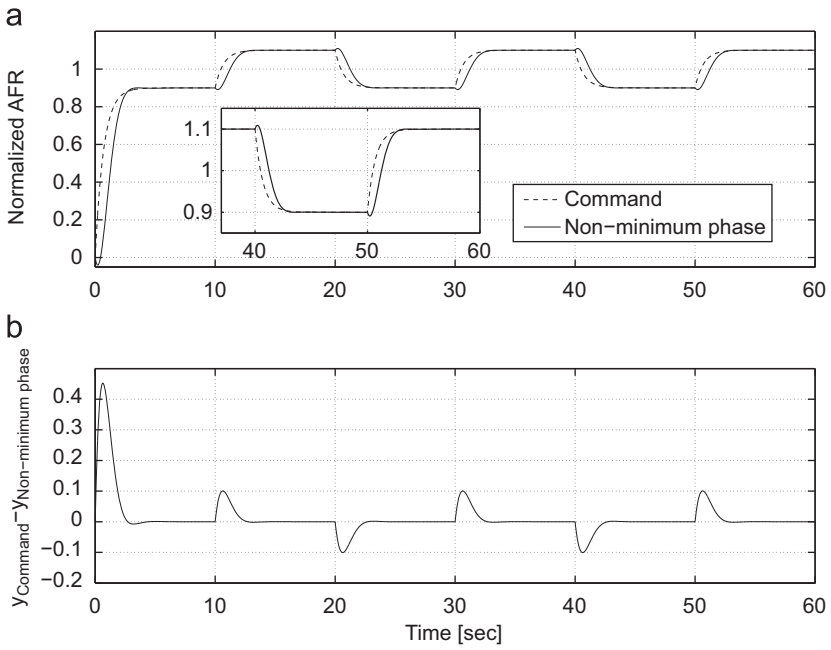

Fig. 5. (a) AFR output for the engine as a non-minimum phase system with a constant delay $\tau = 0.5$ s, (b) AFR difference for the command and the non-minimum phase output ($y_{\text{Command}} - y_{\text{Non-minimum phase}}$).

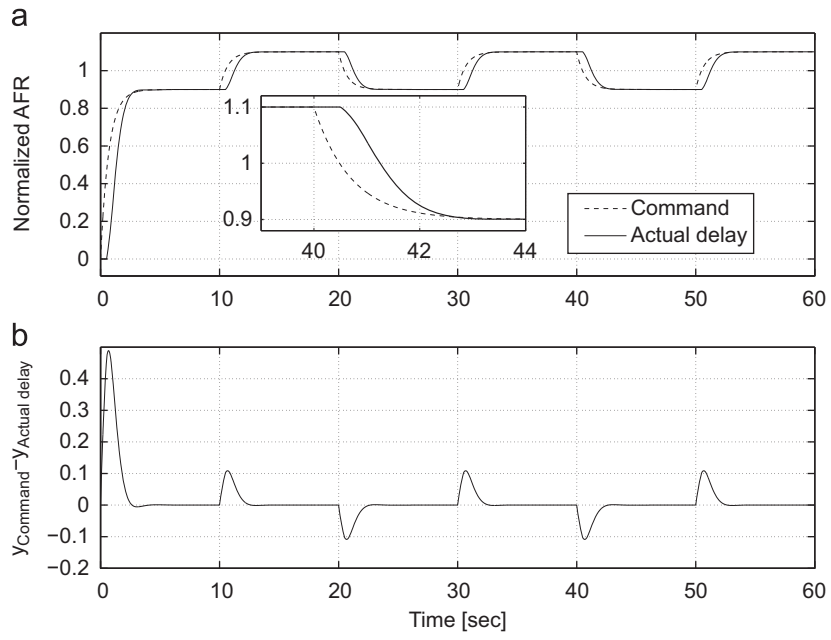

Fig. 6. (a) AFR output with a constant delay $\tau = 0.5$ s for the actual delay and the approximated non-minimum phase system, (b) AFR difference for the command and actual delay ($y_{\text{Command}} - y_{\text{Actual delay}}$).

produces amplitude about 5% of the output. The noise and its effect on the tracking performance in the presence of disturbance are shown in Fig. 11(a) and (b), respectively. It is shown that the control system is able to attenuate the noise effect and enforce the system tracking error close to zero. The control input for the noisy output of the system is illustrated in Fig. 11(c) which shows that the proposed controller with the designed dynamic compensator tracks the predefined tailpipe AFR successfully with good robustness properties in the presence of delay estimation errors, open-loop disturbances, and the UEGO sensor measurement noise.

In a lean-burn engine with large time-varying delay, the objective is to maintain the engine to operate at high AFR. This ensures the high efficiency of the engine and low polluting emission. However, for lean-burn engines new challenges arise due to the lack of conversion efficiency for the TWC to convert produced NO_x pollutants. To tackle this problem, a lean NO_x trap (LNT) module is integrated with TWC to meet standard regulations. The integrated system stores the exhaust NO_x downstream the TWC and releases the trapped gas when it reaches a certain threshold. Simultaneous short-time switching to the rich operation condition converts the released NO_x into non-polluting nitrogen. Consequently, proper switching from lean operation into rich condition and vice versa is necessary to achieve high efficiency of fuel economy and reduced emission levels.

In this paper, the proposed compensator and the controller are employed to track the reference AFR for lean-burn engines. The

main challenge in designing the control system for lean-burn engines is the large delay due to the position of the UEGO sensor after the LNT module. This introduces considerable time-varying delay to τ_g. The additional delay is essentially the time it takes for the gas to be transported to the UEGO sensor. In addition, the engine operating conditions such as the engine speed and air mass flow contribute to the large time delay. In this paper, experimental numerical data collected from a Ford truck F-150 with a V8 4.6 L lean-burn engine with time-varying delay from 0.3 s to 2.7 s (Zhang et al., 2007) is used. To this purpose, the parameter-varying control (18) and the corresponding compensator (19) are employed. Fig. 12 shows the engine speed and air mass flow over a typical Federal Test Procedure (FTP) transient cycle. By using $\alpha = 1.831$ (Zhang et al., 2007) in (3) and having the cycle delay from (2) the overall delay can be represented in Fig. 13. A saturation function with upper limit of 2.7 s has been used to filter out large time delay in the beginning of the engine operation. Fig. 14 shows the closed-loop system performance using the designed controller subject to an open-loop disturbance similar to the one in Fig. 7 and various time delay estimation errors including a 20% underestimation and overestimation. The control exhibits the settling time of 9 s with zero steady state tracking error. It can be observed that for 150 s $< t <$ 170 s (where the time delay is high) with additional estimation error the system exhibits slight oscillations due to the decreased phase margin and thus reduced damping coefficient.

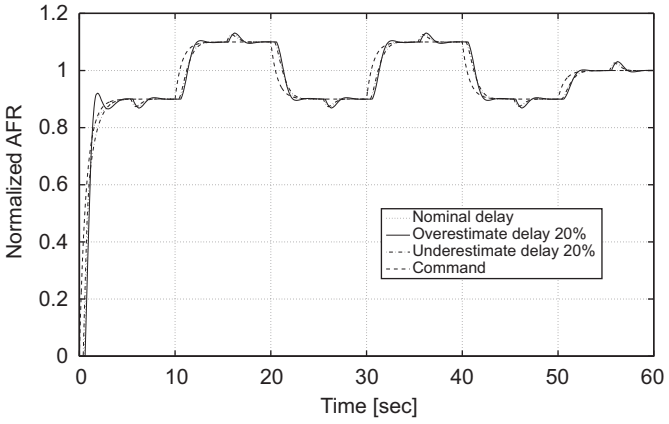

Fig. 9. AFR output of the engine with errors in estimated delay.

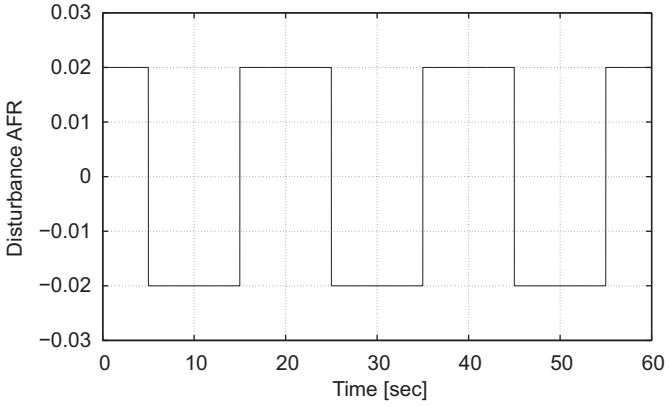

Fig. 7. Open-loop disturbances during the engine operating envelope.

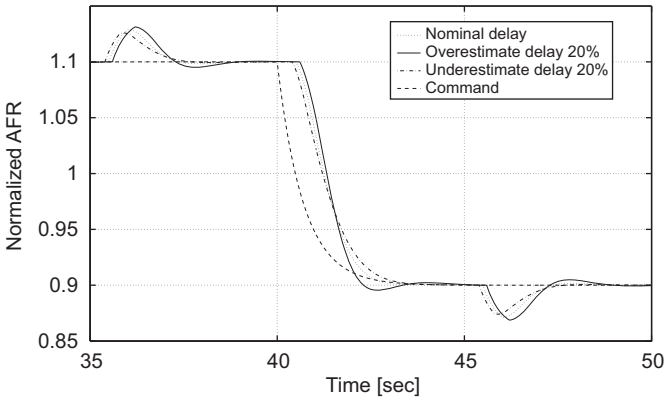

Fig. 10. Detailed view of engine AFR output with errors in estimated delay.

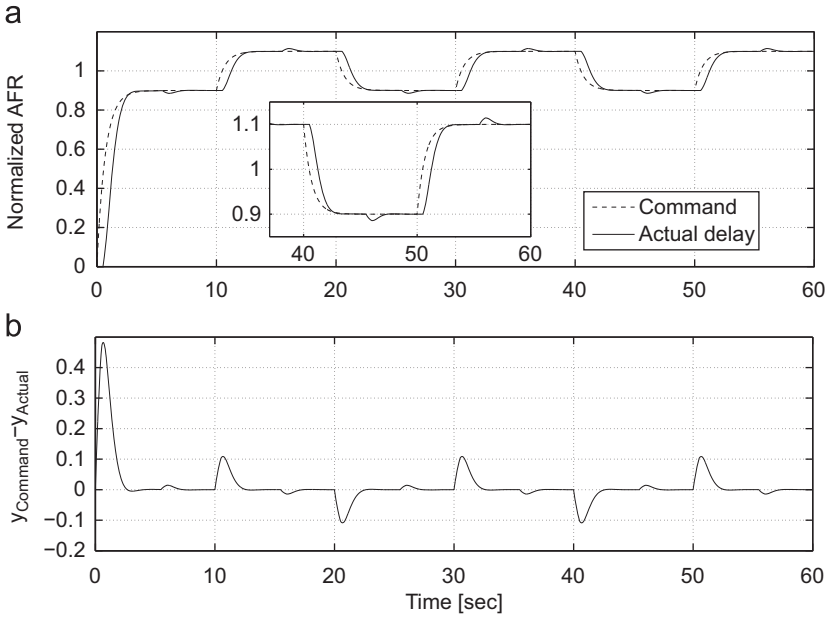

Fig. 8. (a) AFR output of the engine in the presence of an open-loop disturbance with a constant delay $\tau = 0.5$ s, (b) AFR difference for the command and the actual delay output ($y_{\text{Command}} - y_{\text{Actual delay}}$).

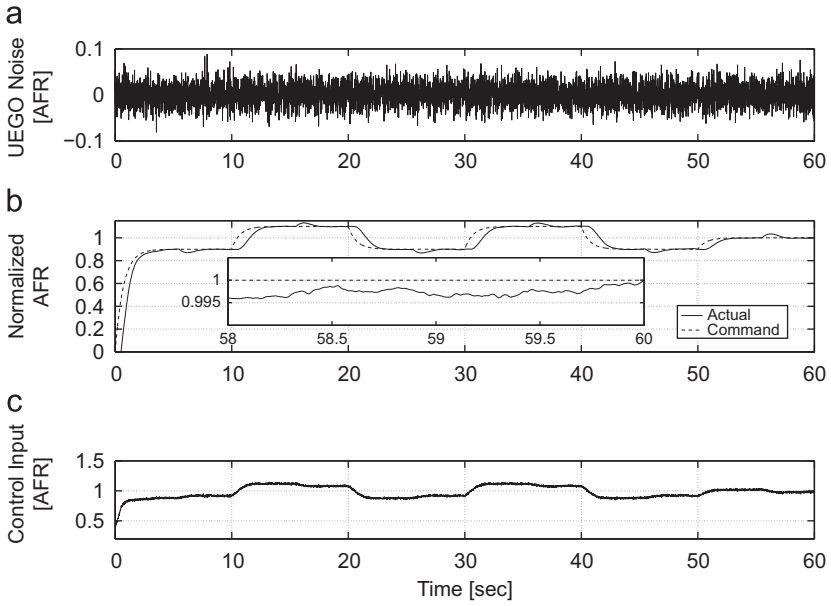

Fig. 11. (a) UEGO sensor noise profile with amplitude of 5% of the output, (b) AFR output of the engine with disturbance and measurement noise, (c) corresponding control input.

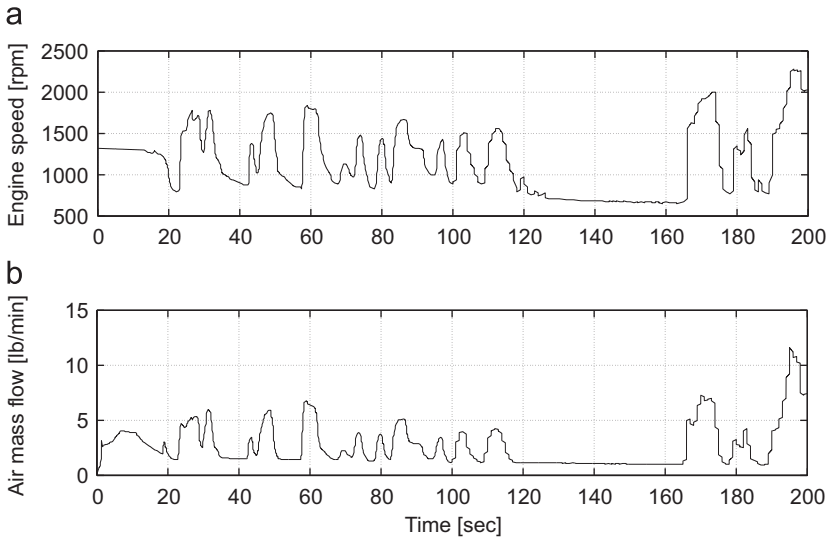

Fig. 12. Engine speed and air mass flow for a typical FTP drive cycle.

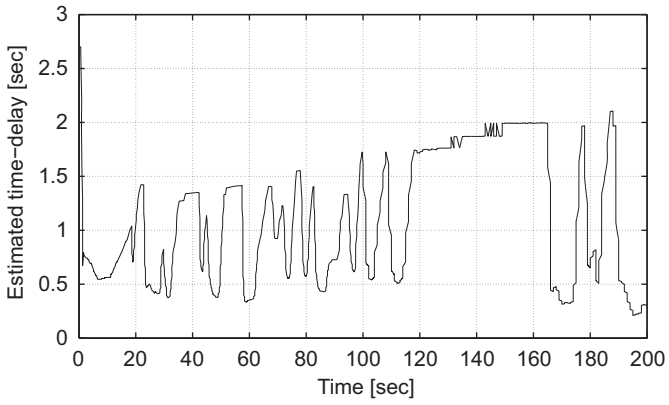

Fig. 13. Estimated time-varying delay for the lean-burn engine.

Fig. 15 demonstrates the time-varying parameters for the compensator and the PID controller gains.

The closed-loop system performance against the UEGO sensor measurement noise and the fuel purge disturbance is illustrated in Fig. 16. The noise is assumed to be a white noise with intensity of 10^{-4} which produces a noise with amplitude of 5% of the sensor output (Fig. 16(a)). Fig. 16(b) shows the closed-loop system performance in the presence of time-varying delay, open-loop disturbance, and the UEGO sensors measurement noise. The magnified graph within Fig. 16(b) shows that the controller has attenuated the noise amplitude and confined the output to ± 0.003 of the reference AFR. It can be observed from Fig. 16(c) that the system has suppressed the noise well for lower delay magnitudes as expected from the Bode plots in Fig. 4. The closed-loop system performance is studied for the fuel-path dynamics according to (1) with $X=0.5$ (half of the injected fuel

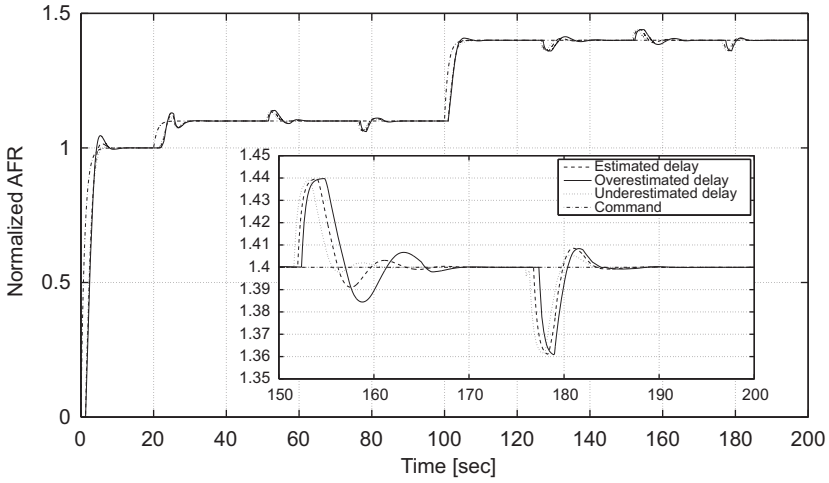

Fig. 14. Closed-loop performance of the time-varying control on the lean-burn engine for multiple time-delay estimation errors.

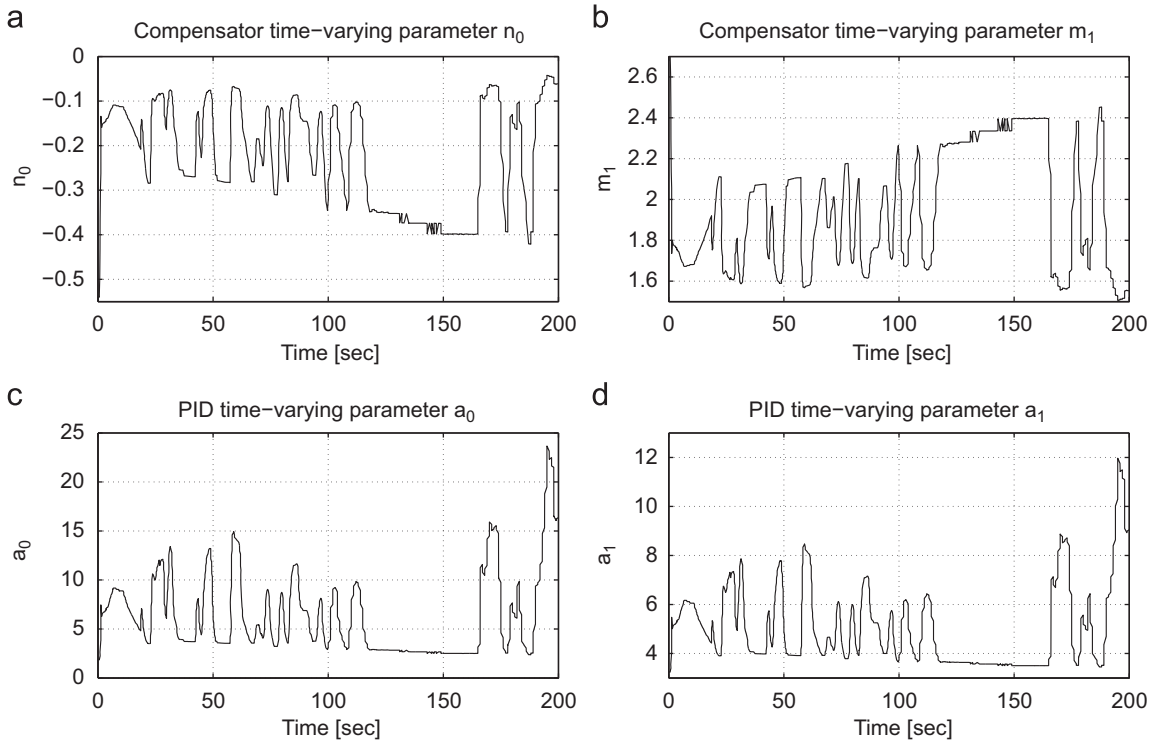

Fig. 15. (a) and (b) Time varying parameters of the compensator, (c) and (d) PID controller time-varying gains.

forms a wet film on the walls) and $\tau_f = 0.1$ (Wu et al., 2009). Fig. 17(a) shows tracking output difference for the case the system is running with and without fuel-path dynamics. The corresponding input difference for the two cases is shown in Fig. 17(b). Although the contributed fuel-path dynamics may help largely to attenuate noise amplitude, it leads to an increase in the control input over transient conditions. However, as a common practice a fuel-path dynamic compensator is included in the system feedforward path which is updated for the fueling system parameters and leads to a decrease in the closed-loop control input. The interested reader is referred to Jones et al. (1994), Wu et al. (2009), and Franchek et al. (2006) for more details.

The presented control approach may be further utilized to obtain a fixed-gain controller by setting the compensator parameters and PID gains for the maximum delay according to Fig. 4. For the lean-burn engine the upper magnitude for the delay ($\tau = 2.7$ s) is used to obtain the compensator parameters and the corresponding controller fixed gains. The closed-loop system performance with the fixed-gain controller in the presence of fuel purge disturbance and the UEGO sensor measurement noise is shown in Fig. 18. Since the bandwidth of the closed-loop system using the designed controller with fixed gains is limited by the maximum delay bandwidth, the system response is more sluggish compared to the parameter-varying controller. In addition, the fixed-gain controller exhibits a lower noise attenuation performance for lower delay values compared to the parameter-varying controller.

5. Conclusion

In this paper, a parameter-varying filtered PID control strategy was proposed for air–fuel ratio control in spark ignition engines

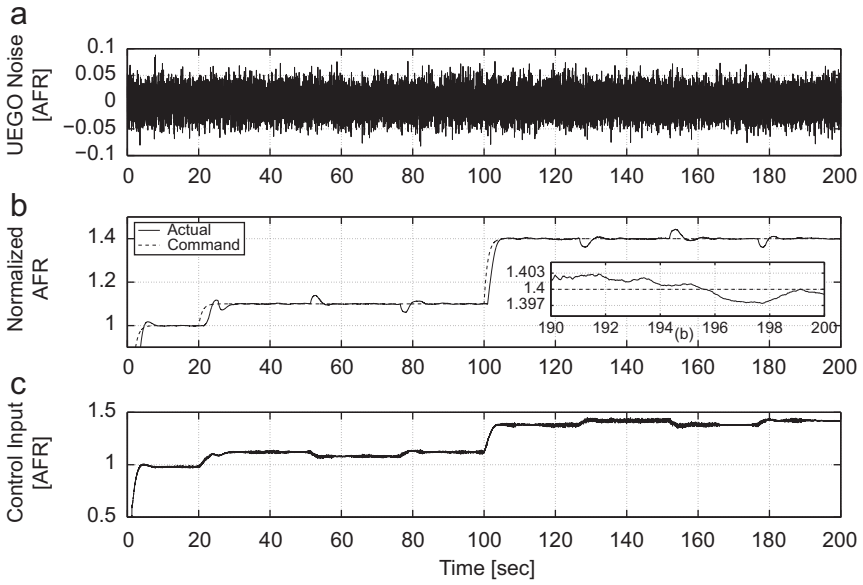

Fig. 16. (a) UEGO sensor noise profile with amplitude of 5% of the output, (b) output tracking for the time-varying delay in the presence of noise and disturbance, (c) corresponding parameter-varying control input.

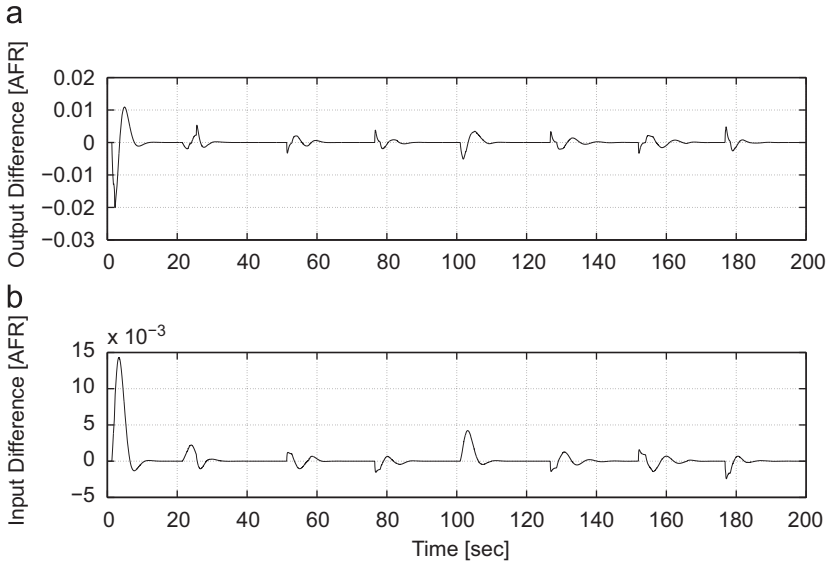

Fig. 17. (a) Output tracking difference with and without fuel-path dynamics for the time-varying delay in the presence of disturbance, (b) the difference in the corresponding parameter-varying control input.

with time-varying delay in the control loop. The engine dynamics with time-varying delay was estimated by the Padé approximation that resulted in a parameter-dependent non-minimum phase system. The system dynamics was further represented in the normal form to investigate the unstable internal dynamics of the engine. A parameter-varying dynamic compensator with parameters explicitly depending on the delay was then constructed based on the unstable internal states of the non-minimum phase system and the tracking error for the engine normalized AFR. The proposed compensator was shown to be able to regulate the closed loop system response against unmatched uncertainties and enable the compensated system to track the reference output with the desired tracking error. Presented parameter-varying dynamic compensator was then used to obtain a controller in the PID form to operate on the filtered tracking error. The closed-loop system performance was evaluated for both port-fuel and lean-burn SI engines with experimental data in the presence of various operating conditions and uncertainties including the overestimated time-varying delays, the fuel purge disturbance, the UEGO sensor measurement noise and the fuel-path dynamics. The results show that the control system is able to reject the effect of the fuel purge uncertainties in the presence of the large engine variable delays for the lean-burn engine as well. Moreover, the control system showed robustness against the various delay estimation errors. The closed-loop system exhibited excellent performance against the UEGO sensor noise and considerably attenuated its effect on the output tracking.

It should be noted that the proposed control approach can be applied to other systems with similar structure. It also does not require additional computational efforts compared to the fixed-gain controllers as only a few multiplications and additions are performed to obtain the varying parameters both for the compensator and the PID controller. Furthermore, the developed parameter-varying control approach can be simplified to obtain

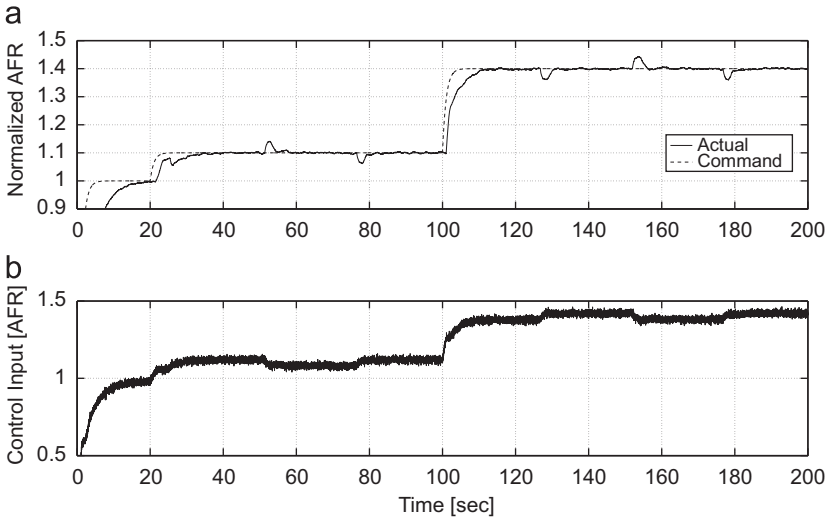

Fig. 18. (a) Output tracking for the fixed-gain controller in the presence of noise and disturbance, (b) corresponding fixed-gain control input.

a fixed-gain controller by setting the compensator and the controller parameters for the maximum delay magnitude. The presented theoretical method along with the simulation results based on the experimental data demonstrate the effectiveness of the proposed approach in designing the AFR control systems for SI engines. The experimental validation will be pursued in a follow-up research.

Acknowledgement

This publication was made possible by NPRP Grant # 08-398-2-160 from the Qatar National Research Fund (a member of Qatar Foundation).

References

Apkarian, P., & Adams, R. (1998). Advanced gain-scheduling techniques for uncertain systems. *IEEE Transactions on Control Systems Technology*, *6*, 21–32.

Aquino, C. F. (1989). *Transient a/f ratio characteristics of* 5 *litre central fuel injection system*. SAE Paper 810494.

Ault, B. A., Jones, V. K., Powell, J. V., & Franklin, G. F. (1994). *Adaptive air–fuel ratio control of a spark-ignition engine*. SAE Paper 940373 (pp. 4082–4090).

Chang, P. H., & Jung, J. H. (2009). A systematic method for gain selection of robust PID control for nonlinear plants of second order controller canonical form. *IEEE Transactions on Control Systems Technology*, *17*(2).

Cho, D., & Hedrick, J. K. (1988). A nonlinear controller design method for fuel-injected automotive engines. *Journal of Engineering for Gas Turbines and Power*, *110*, 313–320.

Choi, S. B., & Hedrick, J. K. (1998). An observer-based controller design method for improving air/fuel characteristics of spark ignition engines. *IEEE Transactions on Control Systems Technology*, *6*(3), 325–334.

Franceschi, E. M., Mucke, R. K., Jones, C. P., & Makki, I. (2007). *An adaptive delay-compensated PID air fuel ratio controller*. SAE World Congress.

Franchek, M. A., Mohrfeld, J., & Osburn, A. (2006). Transient fueling controller identification for spark ignition engines. *ASME Journal of Dynamic Systems, Measurement, and Control*, *128*.

Isidori, A. (1995). *Nonlinear control systems* (3rd ed.). London, UK: Springer-Verlag.

Jones, V. K., Ault, B. A., Franklin, G. F., & Powell, J. V. (1994). Identification and air–fuel ratio control of a spark ignition engine. *IEEE Transactions on Control Systems Technology*, *3*(1).

Kwiatkowski, A., Werner, H., Blath, J. P., Ali, A., & Schulalbers, M. (2009). Linear parameter varying PID controller design for charge control of a spark-ignited engine. *Control Engineering Practice*, *17*, 1307–1317.

Li, Y., Ang, K. H., & Chong, G. C. Y. (2006). PID control system analysis and design. *IEEE Control Systems Magazine*, *26*(1).

Manzie, C., Palaniswami, M., Ralph, D., Watson, H., & Yi, X. (2002). Model predictive control of a fuel injection system with a radial basis function network observer. *ASME Journal of Dynamic Systems, Measurement, and Control*, *124*(4), 648–658.

Pace, S., & Zho, G. G. (2009). Air-to-fuel and dual–fuel ratio control of an internal combustion engine. *SAE International Journal of Engines*, *2*(2), 245–253.

Shkolnikov, I. A., & Shtessel, Y. (2001). Aircraft nonminimum phase control in dynamic sliding manifolds. *Journal of Guidance, Control, and Dynamics*, *24*.

Turin, R., & Geering, H. (1995). Model-reference adaptive a/f ratio control in an SI engine based on Kalman-filtering techniques. In *American control conference* (pp. 4082–4090).

Wang, S., & Yu, D. L. (2007). A new development of internal combustion engine air–fuel ratio control with second-order sliding mode. *ASME Journal of Dynamic Systems, Measurement, and Control*, *129*, 757–766.

Wu, Y.-Y., Chen, B.-C., Hsieh, F.-C., & Ke, C.-T. (2009). *A study of the characteristics of fuel-film dynamics for four-stroke small-scale spark-ignition engines*. SAE paper 2009-01-0591.

Yildiz, Y., Annaswamy, A., Yanakiev, D., & Kolmanovski, I. (2010). Spark ignition engine fuel-to-air ratio control: An adaptive control approach. *Control Engineering Practice*, *18*, 1369–1378.

Yoon, P., Park, S., Sunwoo, M., Ohm, I., & Yoon, K. J. (2000). *Closed-loop control of spark advanced and air–fuel ratio in SI engines using cylinder pressure*. SAE World Congress.

Zhang, F., Grigoriadis, K., Franchek, M., & Makki, I. (2007). Linear parameter-varying lean burn air–fuel ratio control for a spark ignition engine. *ASME Journal of Dynamic Systems, Measurement, and Control*, *129*.